Journal of Physics: Conference Series

Experimental and theoretical analysis of heat transfer in a solar collector storage

Experimental and theoretical analysis of heat transfer in a solar collector storage

Hadi R. Al-Dayyeni[a], Wisam J. Khudhayer[b], Cihan Karatas[c], Mustafa Wahby Kanbar JABER[d], Hasan T. Jalel[e].

[a] The General Company of Electrical Power Systems Rehabilitation, Ministry of Electricity, Baghdad, IRAQ.
[b]Department of Energy Engineering, College of Enegineering / Al-Musayab, University of Babylon, Hillah 51002, IRAQ.
[c] University of Turkish Aeronautical Association, Department of Mechatronics Engineering, Ankara, TURKEY.
[d] Ministry of Higher Education, IRAQ.
[e] State Commission of Dams and Reservoirs Ministry of Water Resources, Baghdad, IRAQ.
Corresponding Author**:** Hadiroomi882@yahoo.com

Abstract The current research includes a practical study of the thermal performance of solar collector integral storage system (ISCS) in which different types of heat exchangers are immersed in its enclosure for comparison. The first type is a straight tube heat exchanger (ST) and the other is a heat exchanger in the form of a coiled tube (CT). The effect of single and double glass layers and fluid flow rates inside the heat exchanger on the natural convection heat transfer of ISCS system is experimentally evaluated by determining the temperature difference of inlet and outlet water through the heat exchanger immersed into the ISCS enclosure, the temperature distribution inside the enclosure, the ISCS efficiency, and the amount of thermal storage during evening times. Three sets of experiments are performed for a different water flow rates (1.0, 1.5, 2.0, and 2.5 Lpm) inside the heat exchanger that is immersed in the thermally insulated enclosure and different glassing layers. The first set represents the presence of a heat exchanger in the form of a straight tube with a single glass was layer on the top face of the enclosure that is called (STSG). The second set uses a coiled tube heat exchanger with a single glass on the upper side of the enclosure and it's named as (CTSG). The last set of experiments is represented by a heat exchanger in the form of a coiled tube with a double glass on the upper face of the enclosure and it's abbreviated as (CTDG). At water flow rate of 1 Lpm, the CTDG exhibited higher temperature difference (28 °C and 19.9 °C than (19.4 and 11.4 °C) for CTSG and (12 and 7.3°C) for STSG during day and night times, respectively. The results reveal that the thermal efficiency (84.5 - 77.8 %) of the (CTDG) case at water flow rate of 2.5 Lpm was higher than the efficiency (68.8 - 56.6%) of (CTSG) case and that (41.7 - 39.7%) of STSG) case during day and night times, respectively. It was also observed that the internal energy exceeds the amount of solar radiation during the day and provides a thermal storage at night due to the complete isolation of the collector. The temperature

measurements near the tube allow the calculation of the Rayleigh number during the heat transfer process, and empirical relationships haves been deduced for each set of experiments between the Nusselt number and the Rayleigh number. Keywords: Integral Collector Storage, Solar Water Heating System, Natural Convection, Heat Exchanger, Single & Double Glazing.

1. Introduction:

Every second, the sun generates immense amounts of energy called (Solar Radiation). The energy is radiated into space as sunlight (47%), ultraviolet rays (7%), and infrared radiation or heat (46%). Only the earth, one part in a billion, intercepts a small portion of this energy but this amount is still enormous. In the past, water must be heated in order to meet the purposes of fires heated water for cooking, cleaning, and bathing. Today, some utility companies are incorporating renewable energy systems of wind and sun into their energy generation. One of the applications of the solar energy is the solar water heaters, some of the solar water heaters used the collector as the storage tank without providing pump to circulating the water in the collector, where depended on the natural convection process. The heat transfer mechanism in the collector and immersed heat exchanger is envisioned as the interaction of negatively buoyant plumes developed in the heat exchanger boundary layer and a large-scale buoyant flow within the core of the collector storage. The magnitude of the incoming solar radiation, thermal stratification within the integral collector storage (ICS) geometric parameters (aspect ratio, inclination of the enclosure, and the placement and relative size of the heat exchanger) will determine the extent of mixing in the collector storage fluid [1]. The natural convection is a mechanism, or type of heat transport, in which the fluid motion is not generated by any external source (like a pump, fan, suction device, etc.) but only by density differences in the fluid occurring due to temperature gradients. In natural convection, fluid surrounding a heat source receives heat and becomes less dense and rises due to the thermal expansion, then the colder fluid above moves to replace it. Eventually, the colder fluid is heated and the process continues, forming a convection current; this process transfers heat energy from the bottom of the convection cell to top. The driving force for natural convection is buoyancy, a result of differences in fluid density, and thus the presence of a proper acceleration such as arises from resistance to gravity, or an equivalent force (arising from acceleration, centrifugal force or Coriolis Effect), is essential for natural convection. For example, natural convection essentially does not operate in free-fall (inertial) environments, such as that of the orbiting International Space Station, where other heat transfer mechanisms are required to prevent electronic components from overheating. Natural convection has attracted a great deal of attention from researchers because of its presence both in nature and engineering applications. In nature, convection cells formed from air raising above sunlight-warmed land or water are a major feature of all weather systems. The convection is also seen in the rising plume of hot air from fire, plate tectonics, oceanic currents (thermo line circulation) and sea-wind formation (where upward convection is also modified by Carioles forces). In engineering applications, convection is commonly visualized in the formation of microstructures during the cooling of molten metals, and fluid flows around shrouded heat-dissipation fins, and solar ponds. A very common industrial application of natural convection is free air cooling without the aid of fans: this can happen on small scales (computer chips) to large scale process equipment [2-5]. The ICS is a batch type system in which the household water is directly heated by the sun and storage tanks serve as solar collectors. Batch water heaters were passive devices wherein the hot water was supplied to a point of usage by using the pressure of water in houses or storage tanks from the solar heated tank 0f all the different solar water heaters, the most widely designed and used by homeowners are batch systems. They are less costly, particularly when they are residence, are often made of recycled material, and have several

components. Usually, the batch system composed of 1 or more tanks covered with black & sealed in the insulated enclosure, with the glazed side cover facing the sun, shown in Figure (1).

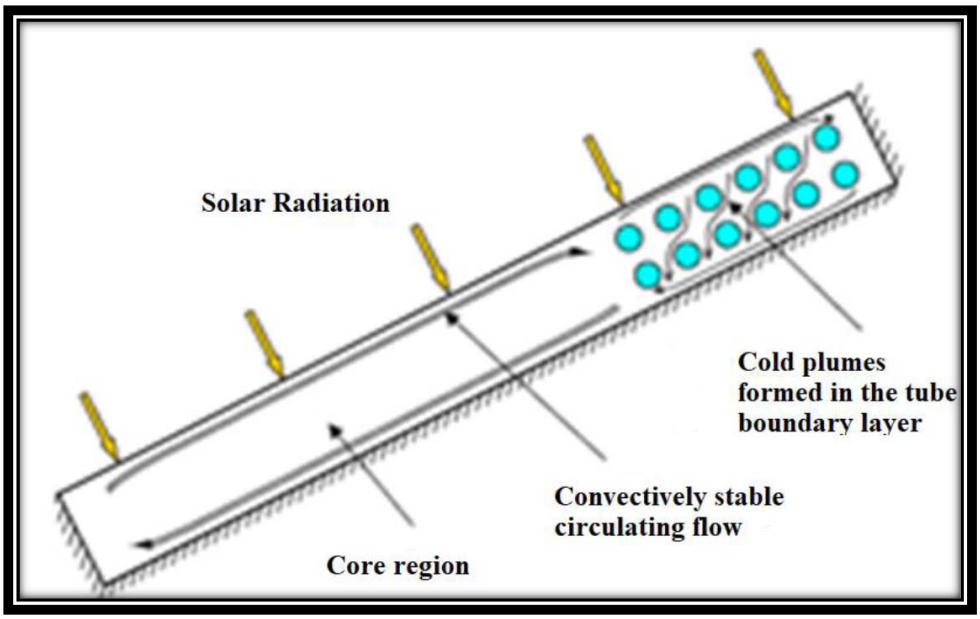

Figure (1): Flow in the collector is envisioned as the interaction of small-scale negatively buoyant plumes developed in the heat exchanger boundary layer and a large-scale circulating flow in the core of the storage fluid [6].

Wei Liu et. al., 2003 [6] studied the heat transfer rates of a single horizontal tube immersed in a water-filled enclosure tilted at 30 degrees. The results serve as a baseline case for a solar water heating system with a heat exchanger immersed in an integral collector storage. The experiments were conducted for isothermal and stratified enclosures with both adiabatic and uniform heat flux boundary conditions. The natural convection flow in the enclosure is interpreted from measured water temperature distributions. The formation of an appropriate temperature difference that drives natural convection is determined. Finally, cempirical orrelations for the overall heat transfer coefficient in terms of the Nusselt and Rayleigh numbers are reduced to the following form NuD= $0.675Ra_D^{0.25}$ for $10^6 \leq$ RaD$\leq 10^8$.

In 2004, W. Liu et. al. [7] evaluated the natural convection heat transfer coefficients for a rectangular array of eight tubes integrated in a thin enclosure of aspect ratio 9.3:1 and inclined at 30 degree. The results for isothermal and stratified enclosures yield the following correlation for the overall Nusselt number: NuD= $(0.7286\pm0.002)RaD^{0.25}$, $4.0X10^5$<RaD<$1.4X10^7$. The flow field in the enclosure is inferred from measured temperature distributions. The temperature difference that drives natural convection is also determined. The results extend earlier work for the case of a single tube and provide limiting case heat transfer data for a tube bundle that occupies the upper portion of the collector storage. In comparison with Nusselt numbers for a single tube, the larger Nusselt numbers in the tube bundle are attributed to stronger fluid motion within the bundle and a larger momentum in the approaching flow from the lower region of the enclosure and higher overall circulation rates.

Later on, W. Liu et al., 2005, [8] studied the natural convection in an enclosure that represents an integral collector storage system (ICS) with an immersed tube-bundle heat exchanger. The heat transfer

coefficients for bundles of 240 tubes contained in a thin enclosure of aspect ratio of 9.3:1 and inclined at 30 degree to the horizontal are obtained for a range of transient operating modes and pitch-to-diameter ratios of 1.5, 2.4, and 3.3. The Results for isothermal and stratified enclosures yield a correlation for the overall Nusselt number NuD = (2.45±0.03)〖Ra〗_D^0.188 , 230<RaD<9800. The characteristic temperature difference in the Rayleigh number is that between the average water temperature within the bundle and the tube wall temperature. It was found that Nusselt numbers are three times larger than those for a similarly configured single-tube and an eight-tube bundle. This increase is attributed to stronger fluid motion within the bundle and higher overall large-scale circulation rates in the enclosure. On the other hand, the double glazing arrangments were found to efficenctlt reduce top loss heat transfer coefficient and improve heat transfer of the conventional solar flat plate collector. The modified solar collector has installed at a latitude angle of 12 degree facing towards north-south directions. The experiments were carried out in thermosiphon principle from 10:00 to 16:00 hrs. The results showed that over all top loss heat transfer coefficient has marginally reduced and collector efficiency 68% obtained. The flow pattern also studied using CFD analysis [9].

H.Vettrivel and P.Mathiazhagan, 2017 [10], performed an experimental study to reduce the overall top loss heat transfer coefficient and improve the solar collector efficiency. A double glaze system was introduced and optimized the space between the absorber plate to glass cover (1) and glass cover (2) were considered to analysis the overall top loss heat transfer coefficient (Ut). The single and double glazing solar flat plate collectors were fabricated with same dimensions and installed at a latitude angle of 12 degree facing towards N-S direction. The experiment were carried out between 10.00 AM to 4.00 PM with thermosyphonprinciple. The result showed that the efficiency of double glazing is higher compared to single glazing system with same solar intensity. The higher efficiency is attributed to the reduction in the overall top loss heat transfer coefficient in double glazing systems.

Finally, J. Manikandan and B. Sivaraman, 2016 [11], evaluated experimentally the performance of single glass flat plate solar water heater (SGFPSWH) and double glazed flat plate solar water heater (DGFPSWH). The galvanized iron plate of 1.42 x 0.7 m2 size was employed as flat absorber plates. A glass plate of similar size was used as top cover for SGFPSWH and two glass plates of same size with a gap of 2 cm were used for DGFPSWH the glass plates used as protection for heat loss from absorber plate to atmosphere. Performance of SGFPSWH and DGFPSWH at different mass flow rates (0.0041, 0.0083, 0.0125 kg/s) were investigated and reported. The thermal efficiency is found to be higher for DGFPSWH compared to SGFPSWH. Based on the above literature, it can be clearly seen that there is few studies focused on evaluating the performance of the integral solar collector storage systems (ISCS) and more in depth investigation is required. Thus, it is necessary to evaluate the thermal performance of ISCS systems using different configurations of heat exchangers that is immersed into its slanted, thermally insulated enclosure. Furthermore, an experimental study is also required to demonstrate the effect of single and double glazing layers of the ISCS enclosure on the heat storage capacity as well as heat transfer by natural convection of the solar water heating system from the enclosure to the heat exchanger at the discharge.

2. Experimental Analysis

2.1 Experimental Setup

The experimental investigation is carried out to evaluate the effect of heat exchangers types (straight tube and coiled tube) immersed in a storage enclosure as well as the single and double glazing factor of the enclosure on natural convection heat transfer in solar water heating systems. To meet these experimental objectives, a accustom-made apparatus is designed and installed as shown in fig. (2) and a detailed experimental procedure is presented.

Figure (2): The ISCS experimental apparatus.

The enclosure is a rectangular Galvanizes sheet iron (corrosion resistible) with thickness of 1.5 mm. The internal dimensions of the enclosure are 122 cm (width) × 94 cm (length) × 11 cm (depth). The tope side (front plate) of the enclosure is a removable door through which the heat exchanger and instrumentation are mounted. The ports enclosure (0.5 mm diameter) for insertion of thermocouples are located along the bottom face. An additional Port with a diameter of 25 mm is used to drain the enclosure. The big upper face is used as a base of the glass facing solar rays. The internal surface of the enclosure is painted by a black paint that absorbs the waves of solar radiation and reflects the long waves. Figures (3) and (4) show the storage enclosure.

Figure (3) Storage enclosure**.**

Figure (4) A close view of the base position of the glass layer in the enclosure.

Two heat exchangers are used. The first heat exchanger is a straight tube and the second model is a coiled tube. The tubes of heat exchanger used in the present research are made from cupper material (according to good thermophysical properties) with thermal conductivity of386 W/m.^{o}C for each heat exchanger types. The straight tube configuration consists of a horizontal and two vertical tubes mounted into the enclosure. The horizontal tube is 1000 mm (long) × 25 mm (outer diameter) × 23 mm (inner diameter) and each vertical tubes is 11.6 cm (long) × 25 mm (outer diameter) × 23 mm (inner diameter). The coiled tube configuration consists of a horizontal coil tube and two vertical tubes mounted inside the enclosure. The horizontal tube is 1000 mm (long), diameter of roll is 80 mm, and the outer and inner

diameter of pipe of coil are 9.2 mm and 8.7 mm respectively. Each vertical tubes is 11.6 cm (long) and the outer and inner diameter are 9.2 mm, 8.7 mm respectively as shown in Figures (5) & (6).

Figure (5) Straight tube.

Figure (6) Coiled tube.

2.2 Temperature Measurements

Twenty one Ports with a diameter of 5 mm are distributed at the bottom face of enclosure for insertion of thermocouples fig. (7) inside the enclosure to measure the temperature of water at different points from T1 to T21.

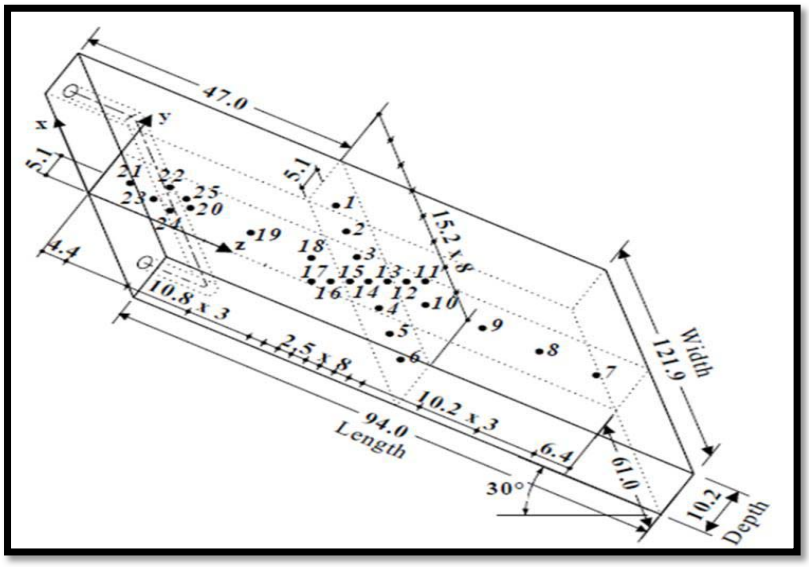

Figure (7) Horizontally Distribution of thermocouples in the mid (y-z) plane(x = 0)

The water temperatures (T22:Ts1 and T24:Ts2) surrounding the tube heat exchanger are measured using two thermocouples probes placed at (180˚) increment (1.2 cm) on the outside wall of the tube. To measure wall temperature of the tube, two thermocouples (T23:Tw1 and T25:Tw2) are fixed at (180˚) increment in (1.1 mm) deep on the tube wall as shown in Figure (8).

Figure (8) Locations of thermocouples for measuring water temperature surrounding the tube heat exchanger.

Two thermocouples are used to measure water temperature at inlet (Ti) and outlet (T_o) water flows inside the tube heat exchanger and. One thermocouple is used to measure the following: the surrounding temperature (T_a), the temperature of enclosure from bake (T_p), the temperature of insulation (T_{ins}), the temperature of first glass (T_{go}), and finally the temperature of second glass (T_{gi}).

2.3 Experimental Procedure

Before running the experiments, the following preparations were carried out as follows: the (ISCS) was filled with de-ionized water and it was oriented to south (using a compass) with a tilt angle of (β=45°) in Baghdad at (33.2° latitude) and (44.3° longitudes). The pump is connected from two sides, exterior from the lower of storage tank and interior to flow meter and then to solar collector to ensure that the flow rate is not changed. The thermocouples were connected to temperature recording device for measuring the temperatures at different points during the experiments. At this stage, the experimental setup is ready to proceed with the following three groups of experiments as shown in fig. (9).

1- Heat exchanger (straight tube) with single glass layer of the enclosure (STSG).
2- Heat exchanger (coiled tube) with single glass layer of the enclosure (CTSG).
3- Heat exchanger (coiled tube) with double glass layer of the enclosure (CTDG).

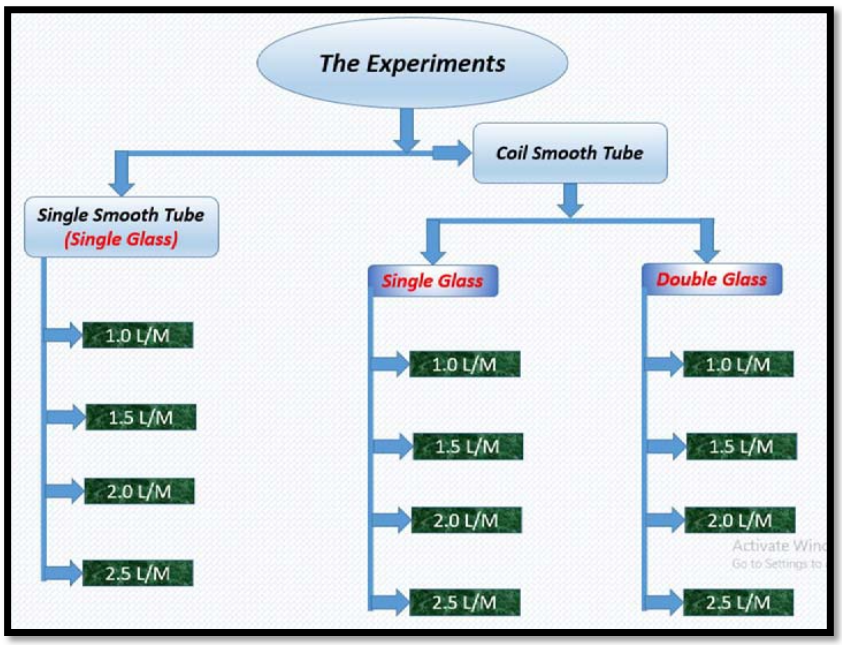

Figure (9) Schematic Diagram of Experiments Study**.**

3. Theoretical Analysis

3.1 Heat Rates (Q)

The total heat rate transmitted to the heat exchanger is calculated by:

$$Q_U = \dot{m}\, C_p(T_O - T_i) \ldots\ldots\ldots\ldots\ldots (1)$$

Where

Q_u: Rate of useful energy gained (W)

ṁ: Mass flow rate of fluid flow(kg/sec)

C_p: Specific heat at constant pressure $(J/Kg.K)$

T_i: Inlet fluid temperature of solar collector (°C)

T_o: Outlet fluid temperature of solar collector (°C)

All properties of water are determined at the average temperature

$$T_{ave} = \frac{(T_o + T_i)}{2} \ldots\ldots\ldots\ldots\ldots\ldots (1\text{-a})$$

3.2 Solar Radiation and Internal Energy

The Internal Energy of water inside the enclosure (W) can be calculated from the following equation [12,13]:

$$Q_i = \dot{m}_{En.}\, C_p(\Delta T_{ave-En.}) \ldots\ldots\ldots\ldots\ldots (2)$$

Where:

$\dot{m}_{En.}$: Mass rate of water inside the enclosure (kg/sec)

C_p : Specific heat at constant pressure of water inside the enclosure ($J/Kg.K$)

$\Delta T_{ave-En.}$: Average of temperatures difference inside the enclosure along the period of discharge operation (C)

The internal energy of the water inside the enclosure is the intermediate source that drives the condensed energy to the heat exchanger contained within the enclosure. This energy was provided due to the solar energy applied to the solar collector SCIS during the morning period from sunrise to the moment the discharge process began, and since the collector is isolated from all sides, so the amount of the internal heat of the water increased to reach twice the instantaneous solar energy, which is a stored energy we use for heat exchange [14].

3.3 Thermal Efficiency

The Efficiency depends on the amount of solar energy absorbing by the ISCS system which is then stored and used at need to heat up the water flowing inside the heat exchanger, taking into account the thermal losses from all sides of the collector. The efficiency is evaluated for all cases during the day and night times. The day time shows how efficient is the collector in acquiring the solar radiation, while the efficiency evaluation during night time reflects the storage capacity as well as the thermal efficiency.
In all classic solar water heating collectors (which use a copper sheet painted black and welded to the tube that is used as a heat exchanger) depend on the fact that solar energy is the energy entering the collector because it works to heat the water directly by heating the plate and thus the amount of energy entering is the same as solar energy.

In our current research, a medium was used to store heat during the day times when the drain was not used, and this medium is water inside the enclosure, where this water in an isolated collector is exposed to solar radiation and its temperature rises and remains storing the thermal energy until the start of the discharge. Therefore, the energy entering the collector is the energy stored in the water because the heat exchanger is immersed inside it, so it will be adopted in the efficiency law mentioned through the relationship (3), the internal energy of the water inside the collector is calculated by determining the average temperature difference distributed inside the enclosure [14].

$$\eta = \left[\frac{Energy\ Gaind}{Stord\ Heat}\right] \ldots\ldots\ldots\ldots\ldots (3)$$

where
Energy Gaind (Q_u): Rate of useful energy gained (W) from the equation (1).
Stord Heat (Q_i): Internal Energy of water inside the enclosure (W).

3.4 Nusselt number (Nu) & Rayleigh number (Ra)

Nusselt number can be defined as the ratio of heat transfer by convection to heat transfer by conducting water atoms [15], and it gives an indication of improved heat transfer by free convection of water layers in relation to heat transfer by conduction. The non-dimensional relationship is considered as one of the pillars of the design of the heat transfer systems, which expresses the effectiveness of the system and its response / behavior to heat transfer. The dimensional relationship of free natural heat transfer system expressed by Nusselt number as a function of Rayleigh number.

The Rayleigh number depends on the flow driven by the force of buoyancy, which is produced in the case of heat transfer by natural convection and it is defined as a ratio between the force of buoyancy to the strength of viscosity [16], that is, any raising the water temperatures inside the enclosure leads to a change in the densities of the water layers that works to reduce the viscosity of hot regions, which in turn

to has a high buoyancy force that moves the water layers in a circular motion inside the enclosure. The increase in heat of the layer surrounding the heat exchanger enhances the heat transfer to heat exchanger.

To find the empirical dimensionless relationships, the Statistica program is used. The temperature measurements near the heat exchanger allow the calculation of the Rayleigh number during the heat transfer process, and non-dimensional, empirical relationships have been deduced between the Nusselt number and the Rayleigh number for each group of experiments. The empirical relationships of CTDG are :

$Nu = 0.150474Ra^{0.447055}$ $6X10^5$ Ra $2X10^7$ R= 96.6% (Daytime) .....(4)

$Nu = 6.121Ra^{0.218}$ $2X10^5$ Ra $6X10^6$ R= 92.7% (Nighttime) ….(5)

4. Results and Discussion

4.1 Temperatures Gradient

The temperature difference of the inlet and outlet water through the submerged heat exchanger in the enclosure depends mainly on the flow rate of water entering (to be heated) inside the heat exchanger; the lower the quantity, the greater the heat gained. That is, the average temperature difference will be higher at low flow rate (1 l/min) in all experiments for all studied cases due to longer residence time of water inside the heat exchanger. The double glass layer of the enclosure (CTDG) exhibited higher temperature difference (28 C and 19.9 C) during day and night times, respectively) than (19.4 to 11.4 C) for CTSG and (12 to 7.3 C) for STSG during day and night times, respectively as shown in Figures (10) and (11).

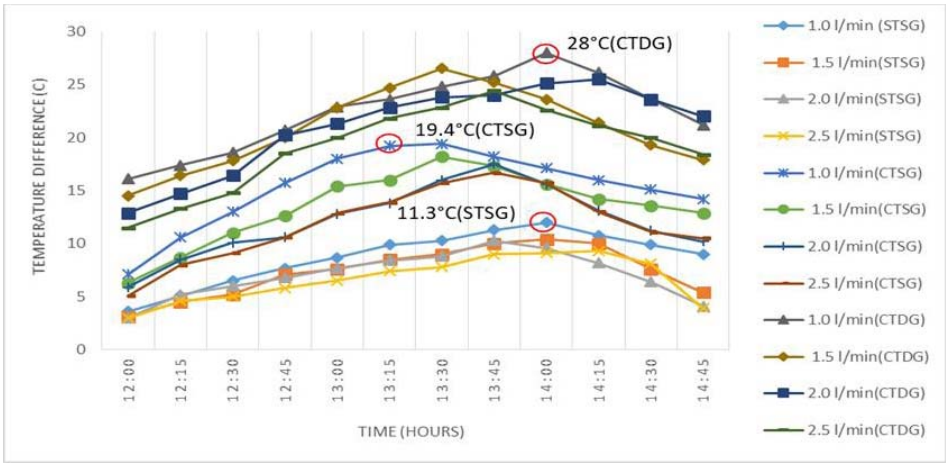

Figure (10) Temperature Gradient with time during the discharge test from 12:00 to 14:45 PM Daytime for all cases STSG, CTSG, and CTDG at different flow rates (1.0, 1.5, 2.0, and 2.5 Lpm).

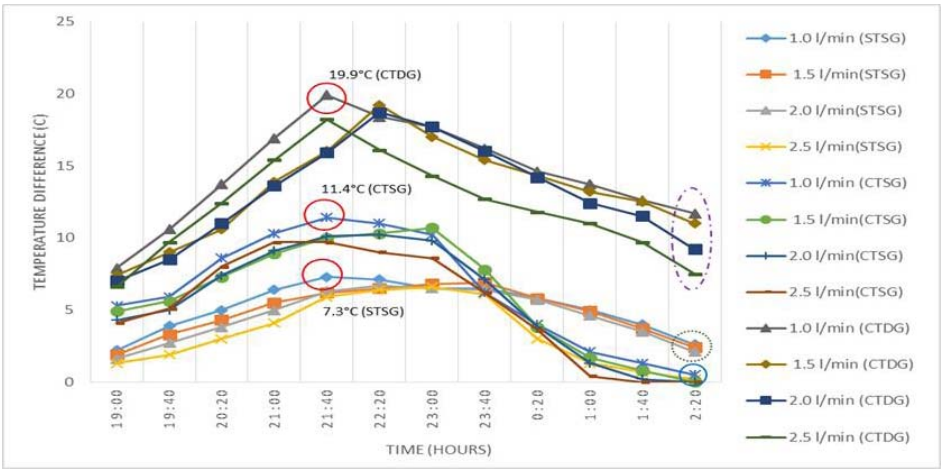

Figure (11) Temperature Gradient with time during the discharge test from 19:00 PM to 02:20 AM Nighttime for all cases STSG, CTSG, and CTDG at different flow rates (1.0, 1.5, 2.0, and 2.5 Lpm).

4.2 Temperature distribution of Enclosure

Since the temperature difference was highest at 1 Lpm flow rate, the temperature distribution will be studied all over the enclosure for all cases at this flow rate. The temperatures were somewhat uniform except near the straight tube within the thermocouple reading (T20). This uniformity is near the back of the enclosure within the two thermocouples reading (T7, T8), where the temperature difference range was (1-3 C) for the water temperature inside the enclosure for all cases. Figures (12,13and 14) show the irregularity for STSG case is less than the CTSG and CTDG cases due to the difference in the temperature surrounding the tube from the temperature of the water entering the tube; the greater the difference, the greater the heat transfer from the enclosure to the tube. This is due to the difference in the density of the water surrounding the tube from another experiment. The change in density leads to a greater buoyancy force, which causes the water to circulate around the tube and the part of the fluid with heavy density (cold water) descends to the bottom, which causes irregularities near the back of the enclosure. Figure (15) reveals that the heat exchange continues with high efficiency when using the case CTDG, and its continuation until after 2 am, and this indicates that the thermal storage in that case is much higher than in other cases due to the use of double glass.

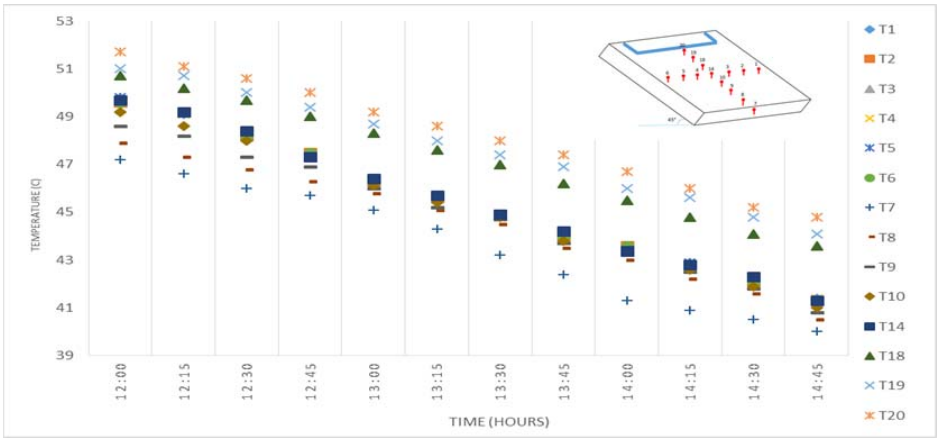

Figure (12) Temperature Distribution (T1-T10 and T18-T20) in the enclosure with time for the STSG case during the discharge at Daytime from 12:00 to 14:45 PM and a flow rate of 1 Lpm.

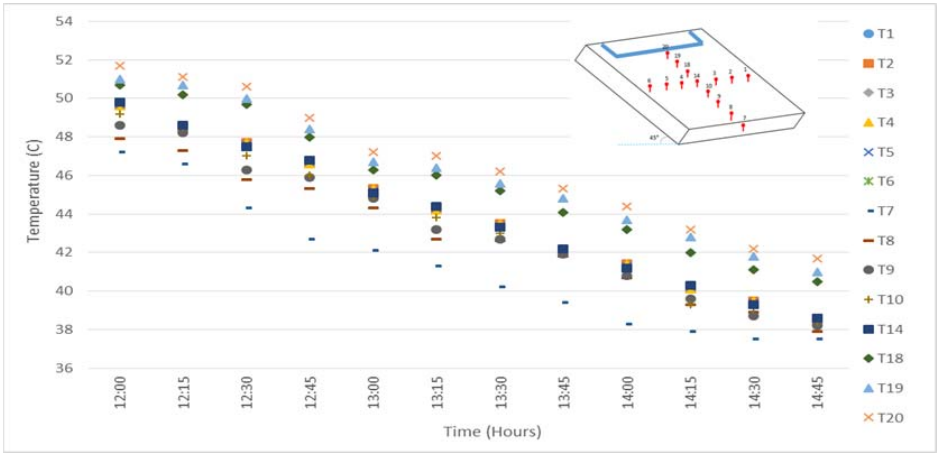

Figure (13) Temperature Distribution (T1-T10 and T18-T20) in the enclosure with time for the CTSG case during the discharge at Daytime from 12:00 to 14:45 PM and a flow rate of 1 Lpm.

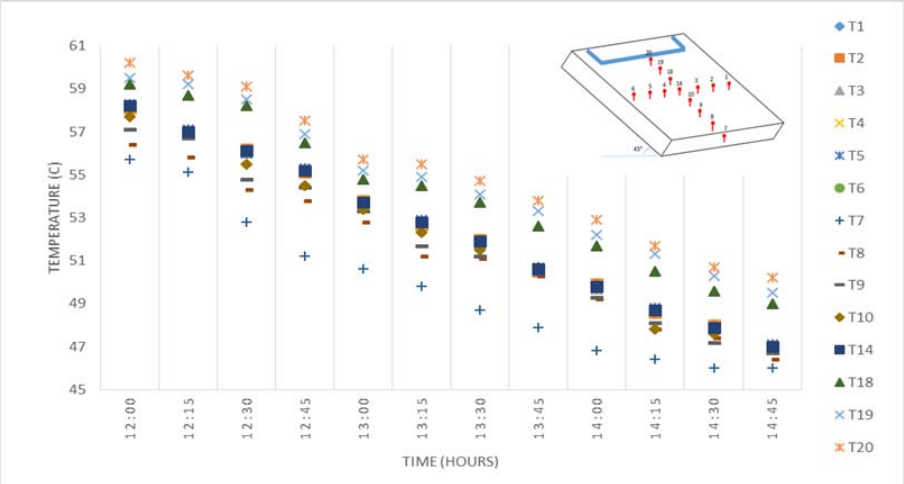

Figure (14) Temperature distribution (T1-T10 and T18-T20) in the enclosure with time for the CTDG case during the discharge at Daytime from 12:00 to 14:45 PM and a flow rate of 1 Lpm.

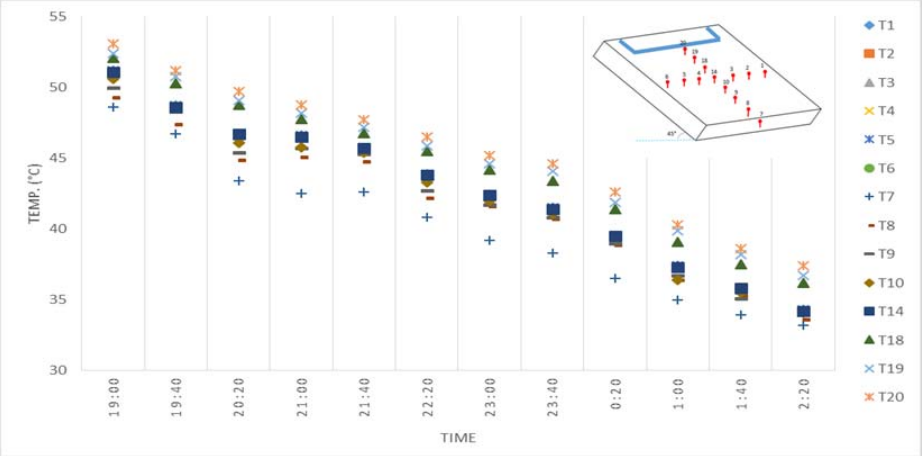

Figure (15) Temperature distribution (T1-T10 and T18-T20) in the enclosure with time for the CTDG case during the discharge at Nighttime from 19:00 PM to 02:20 AM and a flow rate of 1 Lpm.

4.3 Temperatures Distribution near the heat exchanger (Ts1 and Ts2):

Figures (16 and 17) show the temperatures distribution near the heat exchanger for CTDG case. The data indicate a slightly hot area above the heat exchanger and a cold plume heading down from the heat exchanger. It was noted that the measured water temperature below the heat exchanger (The thermocouple Ts2) is (1.5 C) colder than the thermocouple reading above heat exchanger (Ts1) during the day and (0.6 C) at night, and it is (0.1 C) hotter than the water temperature near the heat exchanger (T20) during the day and night times. This indicates that there is a slight gradient in the density of water near the heat exchanger due to the change in temperatures near the heat exchanger and, thus the heat exchange between the enclosure water and the heat exchanger. The temperatures near the heat exchanger are higher by (4 C) during the day and (3 C) at night times, from those that were measured in the middle and bottom part of

the enclosure. This indicates that there is a good gradient of water density in the enclosure due to the temperature change at the top, middle and bottom, which leads to flow down of a cold plume from the tube heading towards the bottom, which works to circulate the water in the enclosure, and the water at the top, sides and bottom of the tube maintains its relative temperature throughout the experiment [17]. It was found that the residence time of the hot zone located in the heat exchanger increases from the case of CTSG to CTDG due to the presence of double glazing layer, which increases the heat transfer rate.

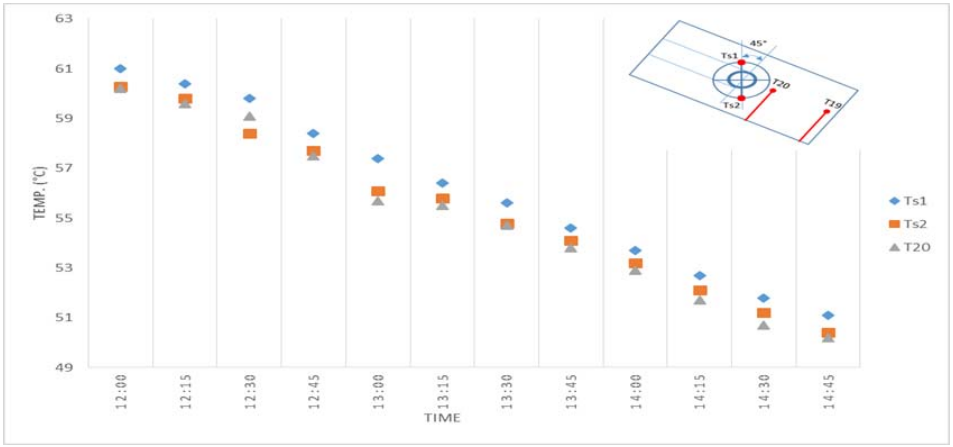

Figure (16) Temperatures Distribution near the heat exchanger (Ts1, Ts2, & T20) with time for the CTDG case during the discharge at Daytime from 12:00 to 14:45 PM and a flow rate of 1 Lpm.

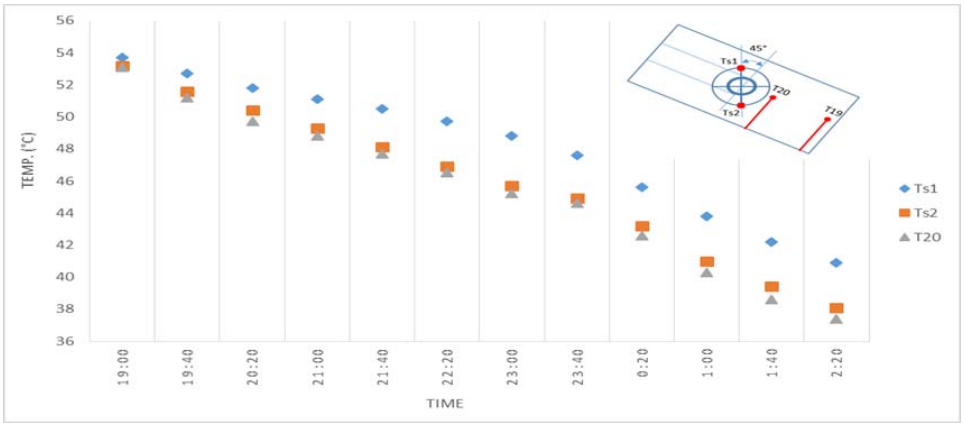

Figure (17) Temperatures Distribution near the heat exchanger (Ts1, Ts2, & T20) with time for the CTDG case during the discharge at Nighttime from 19:00 PM to 02:20 AM and a flow rate of 1 Lpm.

4.4 Temperatures Distribution at the center of the enclosure (T11-T17):

Figure (18) shows the location of the thermocouples (T11-T17) in the middle of the enclosure. These thermocouples have been placed to find out the details of the natural convection heat transfer and how the fluid is effectively circulated with buoyancy force.

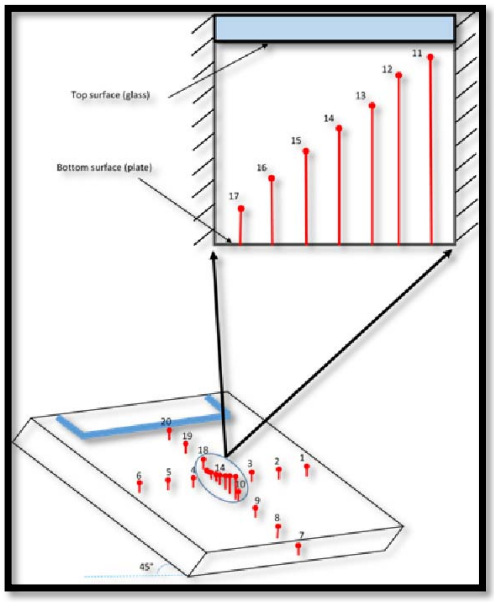

Figure (18) Thermocouples Locations (T11-T17) at the center of the enclosure

Figures (19 and 20) present a graph of the temperature readings of the seven thermocouples (T11-T17) along the horizontal line in the center of the enclosure during day and night times for the CTDG case. It is noticed that the water on the bottom surface (T17) of the enclosure is slightly colder than other locations indicating the heading down of the cold plume to the bottom as the highest temperature difference between the thermocouple readings at the nearest location from the bottom (T17) and the rate of the other six thermocouples (from T11 to T16) is less than (2 C) and the average difference was (1 C).

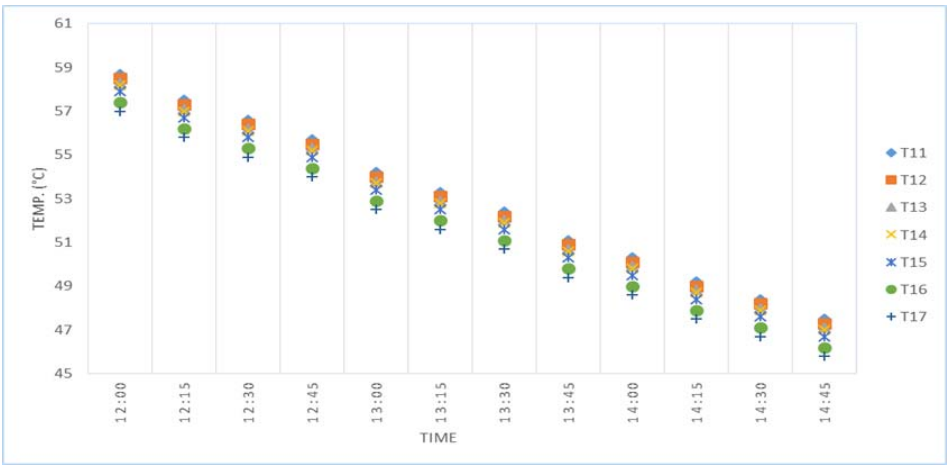

Figure (19) Measured Temperatures at the center of the enclosure (T11 to T17) with time for the CTDG case during the discharge at Daytime from 12:00 to 14:45 PM with a flow rate of 1 Lpm.

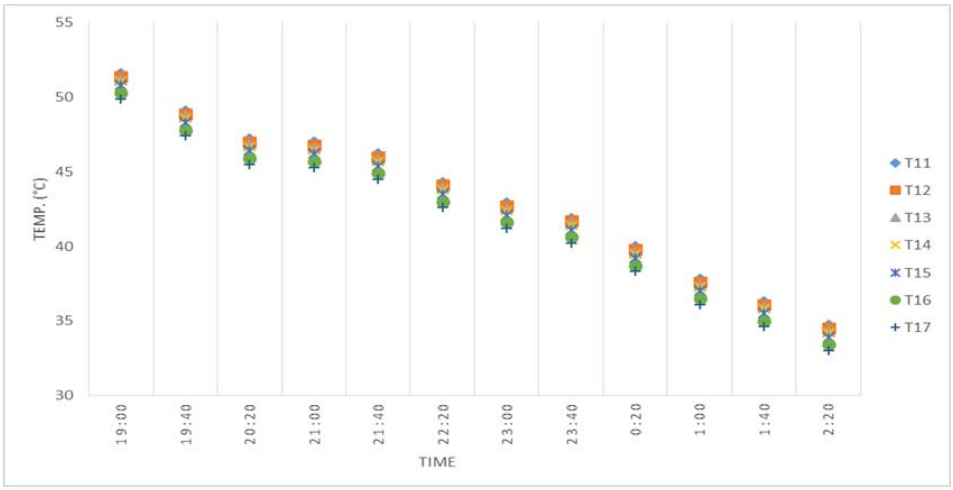

Figure (20) Measured temperatures at the center of the enclosure (T11 to T17) with time for the CTDG case, during the discharge at Nighttime from 19:00 PM to 02:20 AM with a flow rate of 1 Lpm.

4.5 Glass Temperature Distribution:

The temperature distribution of the glass layer for all cases during the daytime at the discharge flow rate of 1 Lpm is presented in Figure (21). The results reveal that the glass temperature for the STSG case is close to the glass temperature of the CTSG and CTDG cases. It should be noted that the temperature of the inner glass is higher than the outer one (8 C) for CTDG case due to the fact that there is resistance from the outer glass that allows the entry of solar rays and prevents the expulsion of heat outside, meaning that it acts as an insulator to prevent heat from escaping outside the collector from the upper face [18], which led to an increase in the temperatures inside the enclosure consequently.

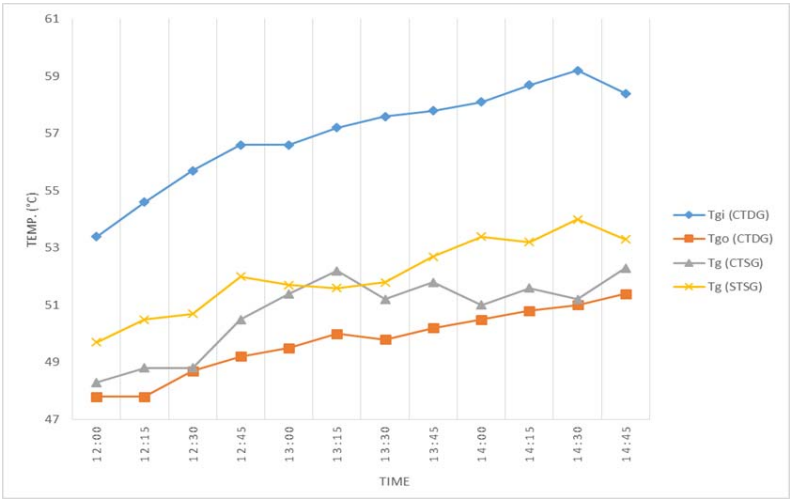

Figure (21) Temperatures of the glass layer for all cases during the daytime with discharge flow rate of (1 Lpm).

4.6 Ambient Temperatures Distribution (Ta):

The variation of the ambient temperatures with time at the discharge water flow rates of (1.0, 1.5, 2.0, and 2.5 Lpm) from 12:00 to 14:45 PM and from 19:00 PM to 02:20 AM of the all cases STSG, CTSG, and CTDG was presented in Figures (22 and 23). The ambient temperatures for all experiments is very close, which makes the comparison relatively fair for all the experiments.

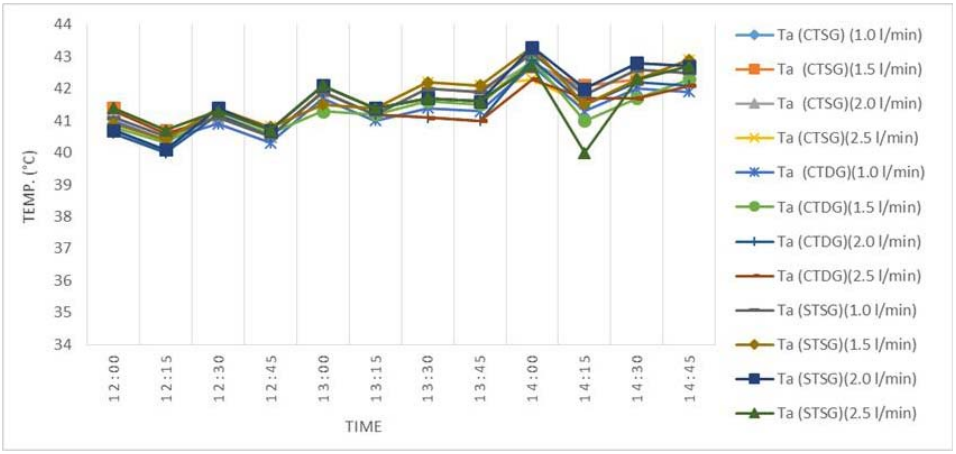

Figure (22) Temperatures of ambient with time for all cases during the Daytime at a water flow rate of (1.0, 1.5, 2.0, and 2.5 Lpm).

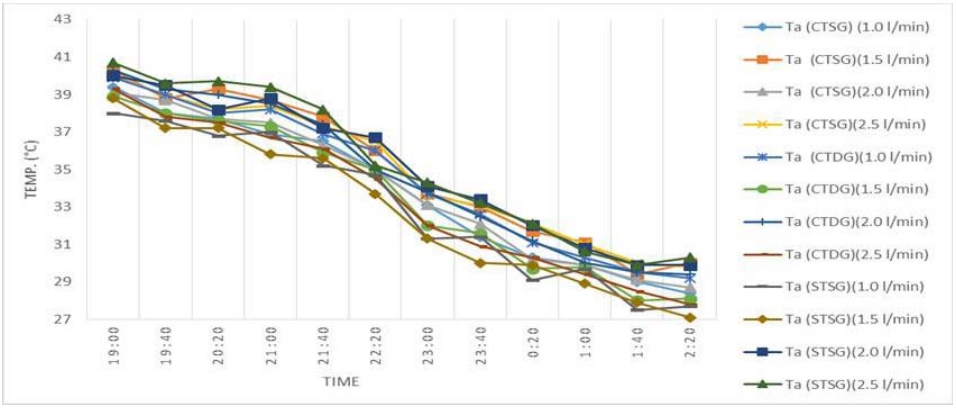

Figure (23) Temperatures of ambient with time for all cases during the Nighttime at a water flow rate of (1.0, 1.5, 2.0, and 2.5 Lpm).

4.7 Heat Rates (Q)

The amount of heat varies from experiment to experiment and from case to case as the amount of heat is higher in all flow rates for CTDG case because the amount of heat gained from solar energy is higher than in the rest of the cases due to the greenhouse effect from double glazing as shown in the Figures below (24 and 25), where it was found that the highest amount of heat is at the flow of 2.5 Lpm for CTDG case (4282 J/s in day & 3194 J/s in night), while CTSG case gives (2930 J/s in day & 1702 J/s in night) and the STSG case provides (1632 J/s in day & 1158 J/s in night).

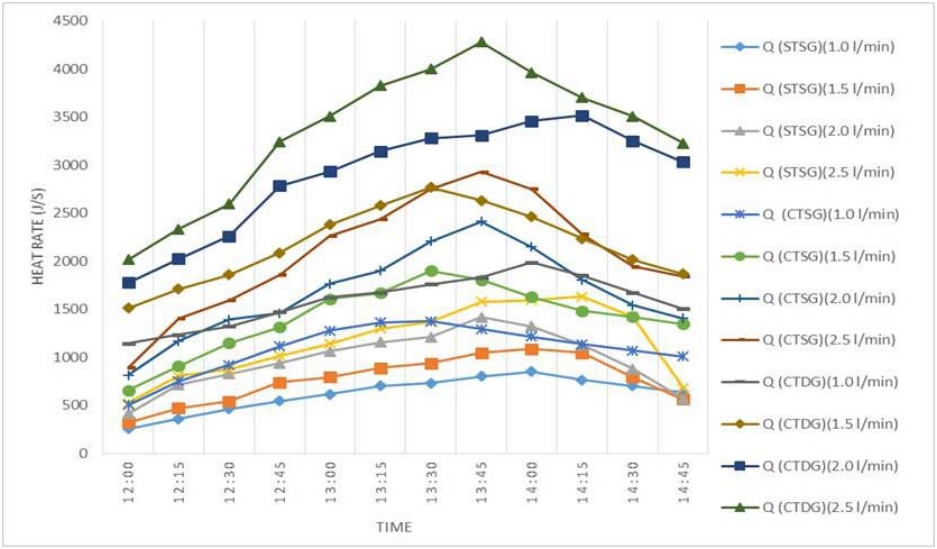

Figure (24) Heat Rates with time for all cases during the Daytime with water flow rates of (1.0, 1.5, 2.0, and 2.5 Lpm).

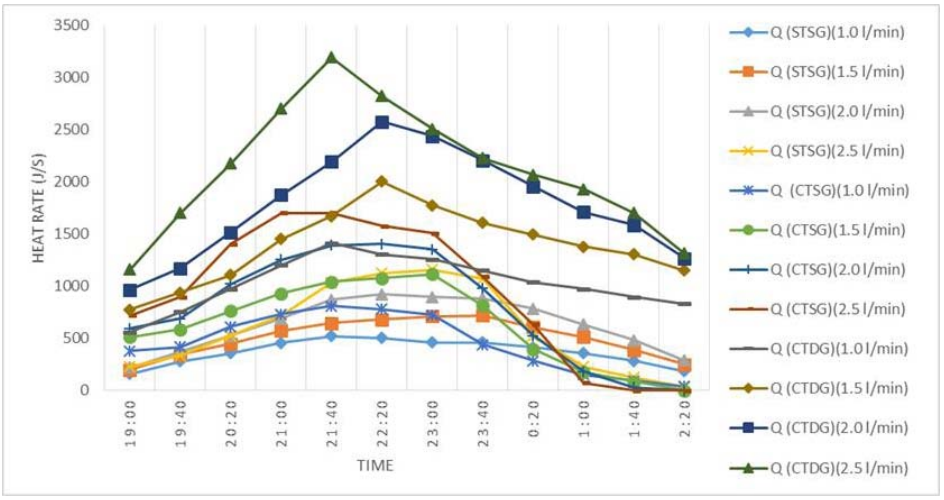

Figure (25) Heat Rates with time for all cases during the Nighttime with water flow rates of (1.0, 1.5, 2.0, and 2.5 Lpm).

4.8 Solar Radiation and Internal Energy

Figures (26,27 and 28) show the amount of solar energy, the temperature difference, and the amount of input energy for the STSG and CTSG cases, where it is observed that the internal energy is close for both cases because they were conducted using single glazing layer and at the same operating conditions. The CTDG case exhibited a higher internal energy than the instantaneous solar energy as well as higher than the internal energy of the two above cases due to the fact that this case uses double glass that makes the

two thermal resistors of the glass work to intensively trap the heat from the sun throughout the morning period.

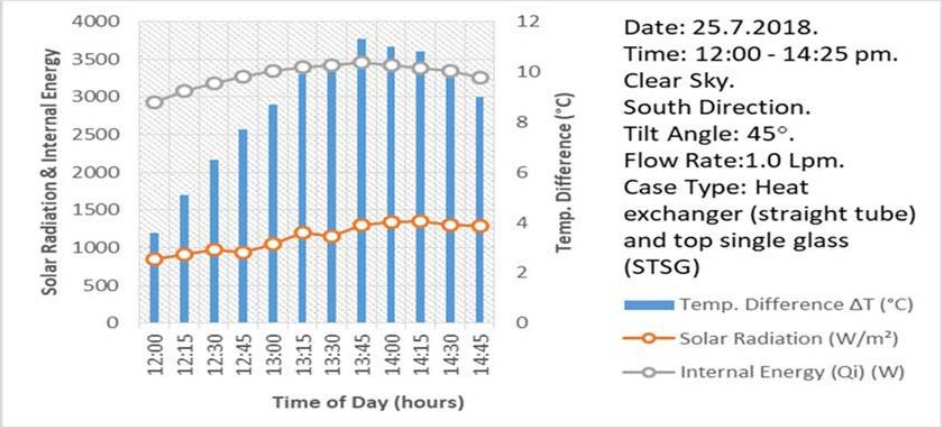

Figure (26) Internal Energy, solar energy, and temperature difference with time on July 25, 2018, during the discharge time with a rate of 1 Lpm for the STSG case.

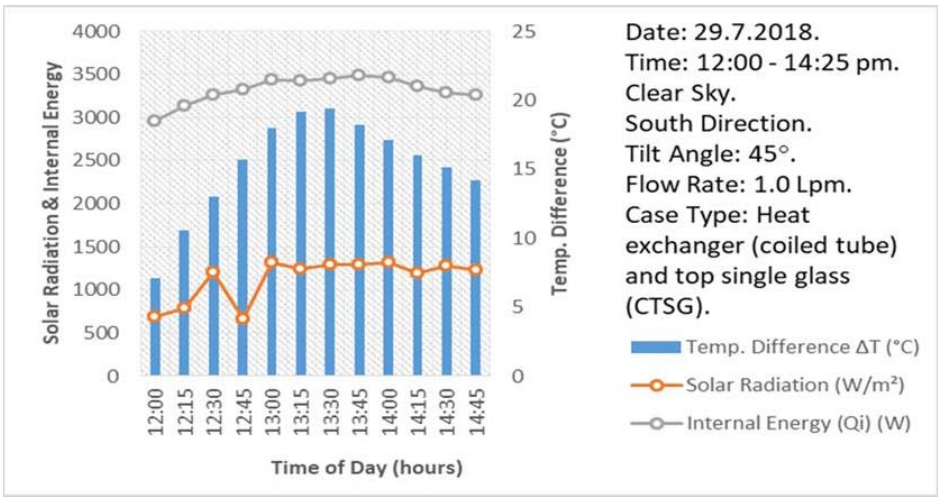

Figure (27) Internal Energy, solar energy, and temperature difference with time on July 29, 2018, during the discharge time witha rate of 1 Lpm for the CTSG case.

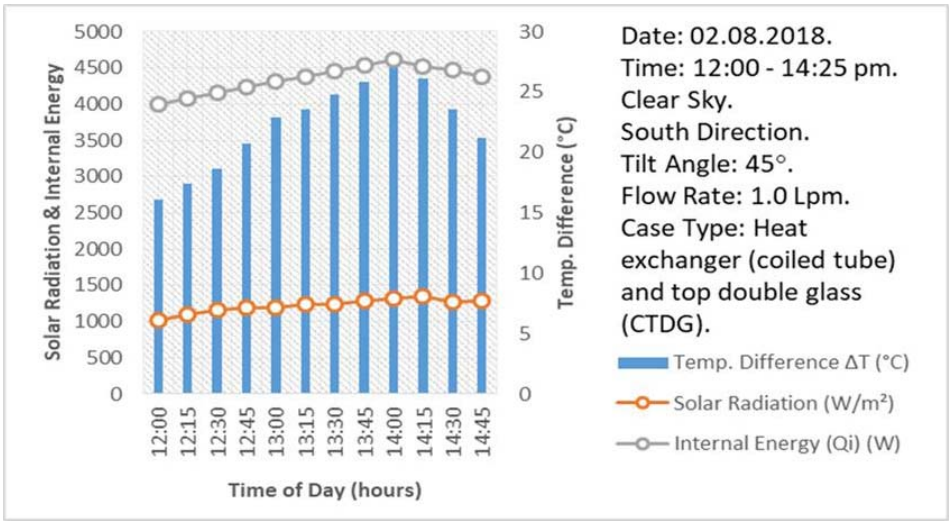

Figure (28) Internal Energy, solar energy, and temperature difference with time on August 02, 2018, during the discharge time with a rate of 1 Lpm for the CTDG case.

Figure (29) shows the internal energy gradient at the discharge process during the evening times, where the internal energy decreases as time passes for all cases due to the absence of solar energy and the heat exchange continues. The internal energy of the CTDG case is higher than the other cases due to the effectiveness of the double glass where the largest energy was stored during the day. It was also found that the continued presence of energy until 02:20 am, and this gives an indication of the large amount of energy stored during the day times. The internal energy of the CTSG case was observed to drop more rapidly than the internal energy of the STSG case, especially after 12:20, due to the enhanced heat transfer rate between the hot water inside the enclosure and the cold water flowing inside the heat exchanger. .

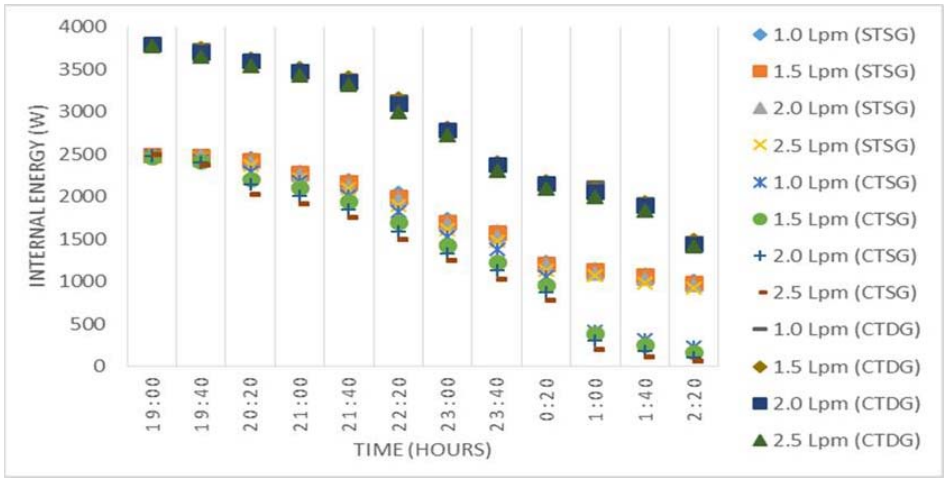

Figure (29) Internal Energy with time on 25,26,27,28,29,30,31 July & 01.02, 03, 04, 05 August, 2018, rspectively during the discharge time with rate of 1.0, 1.5, 2.0, and 2.5 Lpm for all cases. (Nighttime).

4.9 Thermal Efficiency:

From the Figure (30), it is noticed that the efficiency of the coiled heat exchanger with the use of double glass CTDG is higher than in other cases, reaching 84.5% at a flow rate of 2.5 Lpm. This gives an indication that the heat losses were less than the other cases and the internal energy was high. On the other hand, the efficiency of CTSG case was calculated to be 68.8%, which is higher than 41% for STSG case at the flow rate of 2.5 Lpm due to the use of a coiled tube instead of the straight tube heat exchanger.

From Figure (31), it was found that all the cases have thermal storage lasts for varying hours during the evening according to the type of the heat exchanger used. The results reveal that the thermal efficiency (77.8%) of the CTDG case at water flow rate of 2.5 Lpm was higher than (56.6%) for CTSG case and that (39.7%) for STSG case. This gives two impressions: first impression is that the heat storage capacity of the double glass enclosure is higher than single glass, and the second impression is that the heat transfer is better for CTDG case compared to other cases. The decrease in efficiency for all types is due to the absence of solar radiation and the increase in losses due to the low ambient temperatures surrounding the (ISCS) system.

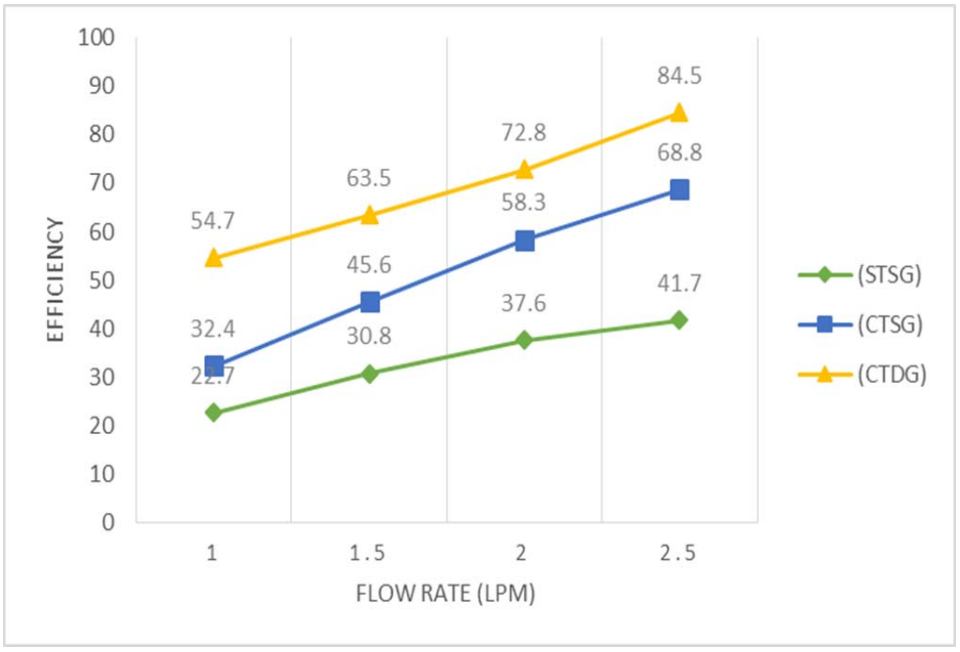

Figure (30) Thermal Efficiency with flow rate of (1.0, 1.5, 2.0, and 2.5 Lpm) during the Daytime for all cases.

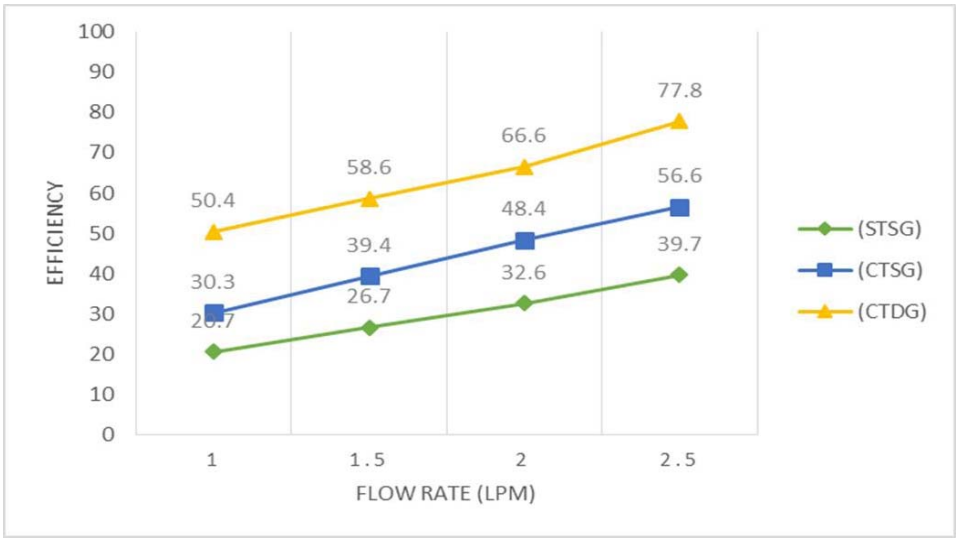

Figure (31) Thermal Efficiency with flow rate of (1.0, 1.5, 2.0, and 2.5 Lpm) during the Nighttime for all cases.

*4.10 Nusselt number (Nu) & Rayleigh number (Ra***)**

The results showed that the highest compatibility between the Nusselt number and the Rayleigh number is was determined for CTDG case as shown in Figures (32 and 33), which show that the Nusselt number increases with the number of Rayleigh, where the resolution ratio was 96.6% during the day and 92.7% at night. This gives a clear indication of the preference for natural convection heat transfer, i.e. whenever the natural convection heat transfer overcomes the conduction heat transfer, it is matched by overcomes of buoyancy forces over viscosity. Whereas, the weakest compatibility between the Nusselt number and the Rayleigh number was observed for STSG case where the resolution ratio was 72.7% during the day and 60.9% at night. In addition to that, the compatibility began to improve for CTSG case where the resolution ratio was 88.5% during the day and 79.9% at night.

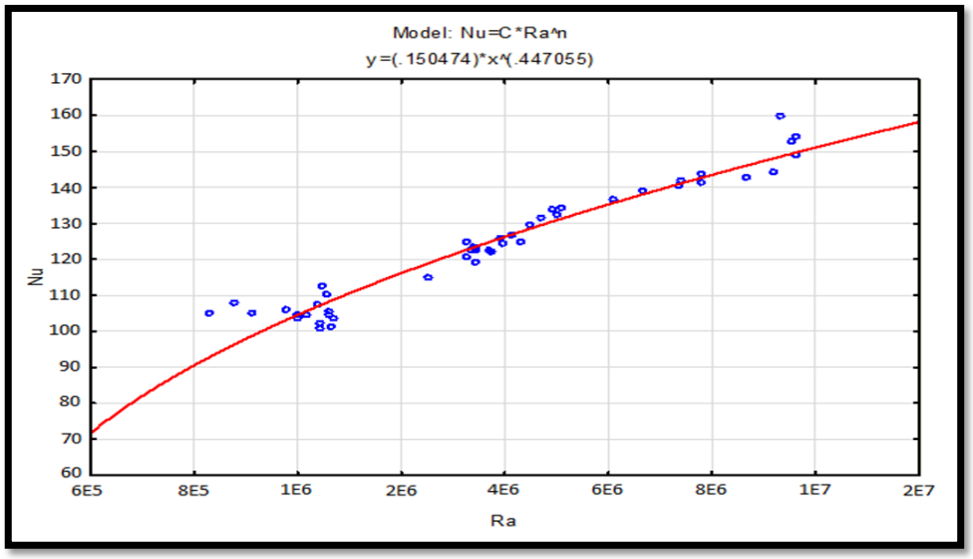

Figure (32) Non Dimensionless relationship of CTDG at Daytime: $Nu = 0.150474Ra^{0.447055}$ $6X10^5$ Ra $2X10^7$ R= 96.6%.

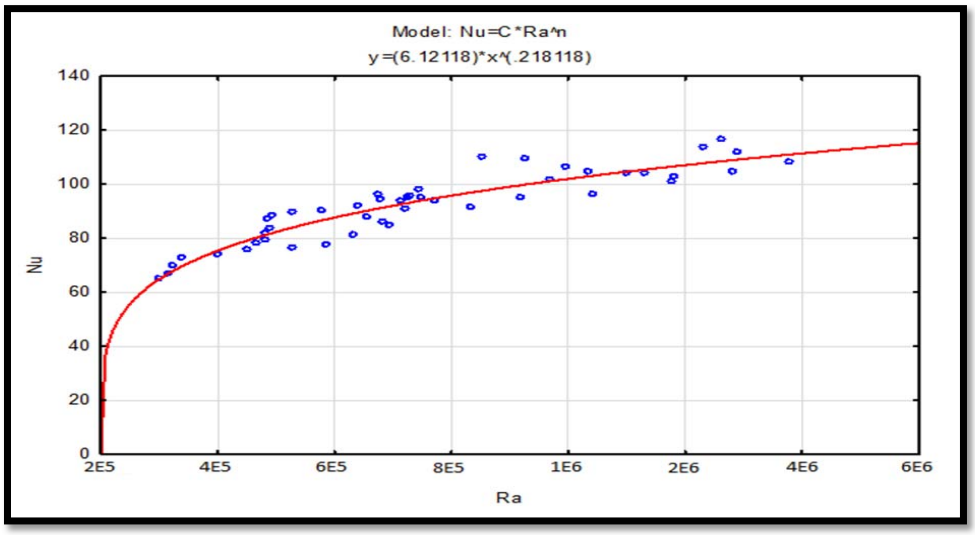

Figure (33) Non Dimensionless relationship of CTDG at Nighttime: $Nu = 6.121Ra^{0.218}$ $2X10^5$ Ra $6X10^6$ R= 92.7%.

5. Conclusions

Temperature measurements of the water in the enclosure allow the characteization of the free-convective heat transfer field from the enclosure to the heat exchanger. The highest temperature difference between the inlet and oulet water through the heat exchanger was reported to be (28 C) and (19.9 C) for

CTDG case during the day and night times, respectivelly, while the STSG and CTSG exhbited a maximum tempretaure difference of (11.3 C – 7.3 C) and (19.4 C – 11.4 C) during day and night times, respectively. The amount of heat transferred to the tube within any level of the initial thermal alignment leads to the descent of a cold feather from the tube to the back of the enclosure, which leads to a rotational movement in the fluid. This helps to fully mix in the middle part of the enclosure. Using water as a medium for heat transfer and storage in this type of solar water heaters gives a high preference over traditional heating collectors. The internal energy of the water inside the enclosure is much higher than the fallen solar energy on the enclosure, and this what raises the donor energy to the heat exchanger and provides thermal storage for evening times. The efficiency of the collector using a heat exchanger in the form of a coiled tube and double glass (CTDG) is higher than those in other cases (STSG and CTSG), which is determined to be 84.5% and 77.5% at daytime and nighttime , respectively.

References

[1] Hadi R. Roomi. “Natural convection from single finned tube immersed in a tilted enclosure”. Journal of Engineering, Vol. 13, No. 3, September 2006.

[2] Donald L. Turcotte; Gerald Schubert. “Geodynamics. Cambridge: Cambridge University Press”. ISBN 978-0-521-66624-4 (2002).

[3] Kays, William; Crawford, Michael; Weigand, Bernhard, “Convective Heat and Mass Transfer”, 4E. McGraw-Hill Professional. ISBN 978-0072990737, (2004).

[4] Jump up to:a b W. McCabe J. Smith ,”Unit Operations of Chemical Engineering”. McGraw Hill. ISBN 978-0-07-044825-4, (1956).

[5] Jump up to:a b c d e Bennett , Momentum, “Heat and Mass Transfer”. McGraw-Hill. ISBN 978 0-07-004667-2, (1962).

[6] W. Liu, J. H. Davidson, F. A. Kulacki, and S. C. Mantell, “Natural convection from a horizontal tube heat exchanger immersed in a tilted enclosure”, International Solar Energy Conference, vol. 16893, pp. 65-74, (2003).

[7] W. Liu, J. H. Davidson, F. A. Kulacki, “Natural Convection From a Tube Bundle in a Thin Inclined Enclosure”, Department of Mechanical Engineering University of Minnesota Minneapolis, Minnesota 55455, 702 Õ Vol. 126, MAY, (2004).

[8] W. Liu, J. H. Davidson, F. A. Kulacki, “Thermal Characterization of Prototypical Integral Collector Storage Systems with Immersed Heat Exchangers” , Journal of Solar Energy Engineering, FEBRUARY 2005, Vol. 127, (2005).

[9] H Vettrivel and P Mathiazhagan “Experimental Investigation of Solar Flat Plate Collector with Double Glazing System” (2016).

[10] H.Vettrivel and P.Mathiazhagan “Comparison Study of Solar Flat Plate Collector with Single and Double Glazing Systems” (2017).

[11] J. Manikandan and B. Sivaraman, “COMPARATIVE STUDIES ON THERMAL EFFICIENCY OF SINGLE AND DOUBLE GLAZED FLAT PLATE SOLAR WATER HEATER”, (2016).

[12] Vulcanic, “Calculatıon of the Power Requıred for Heatıng a Volume of Liquid,” https://www.vulcanic.com/en/heating-volume-liquid/, (2015).

[13] The Engineering ToolBox “Thermal Energy Stored in Heated Water,” https://www.engineeringtoolbox.com/energy-storage-water-d_1463.html, (2009).

[14] T. Li, Y. Liu, D. Wang, K. Shang, and J. Liu, “Optimization analysis on storage tank volume in the solar heating system “, Procedia Engineering, vol. 121, pp.1356-1364, (2015).

[15] Çengel, Yunus A. “Heat and Mass Transfer (Second Ed.)”, McGraw-Hill. p. 466, (2002).

[16] Baron Rayleigh "On convection currents in a horizontal layer of fluid, when the higher temperature is on the underside", London Edinburgh Dublin Phil. Mag. J. Sci. 32 (192): 529–546, (1916).

[17] J. Banaszek, Y. Jaluria, T. A. Kowalewski, and M. Rebow, “Semi-Implicit Fem Analysis of Natural Convection in Freezing Water”, Numerical Heat Transfer, Part A: Applications. vol. 36(5) pp. 449–472, (1999).

[18] H. Vettrivel, and P. Mathiazhagan, “Comparison Study of Solar Flat Plate Collector with Single and Double Glazing Systems”, International Journal of Renewable Energy Research (IJRER), vol. 7(1), pp. 266-274. (2017).